Autophagy and apoptosis: studies on the effects of bisthiosemicarbazone copper(II) complexes on p53 and p53-null tumour cell lines

Journal Name

ARTICLE

Autophagy and apoptosis: studies on the effects of bisthiosemicarbazone copper(II) complexes on p53 and p53-null tumour cell lines

Received 00th January 20xx,
Accepted 00th January 20xx

DOI: 10.1039/x0xx00000x
www.rsc.org/

Franco Bisceglie,[ab] Rossella Alinovi[bc] , Silvana Pinelli[bc], Maricla Galetti[c], Marianna Pioli[a], Pieralberto Tarasconi [ab], Antonio Mutti[c], Matteo Goldoni[c] and Giorgio Pelosi [*ab]

A comparative study between two bisthiosemicarbazones, 2,3-butanedione bis(4,4-dimethyl-3-thiosemicarbazone) and 2,3-butanedione bis(2-methyl-3-thiosemicarbazone), and their copper(II) complexes is reported. The four compounds have been tested on leukemia cell line U937 (p53-null) and on adenocarcinoma cell line A549. The study includes cell viability, cell cycle, morphological changes, assessment of apoptosis, analysis of autophagy, measurement of reactive oxygen species (ROS) and of lipid peroxidation, protein determination, assessment of the expression of p53 and cellular uptake of metal complexes. Tests about the copper uptake under normoxic and hypoxic conditions were also carried out on solid tumour cell line A549. The four compounds under study elicit different effects on the two lines adopted as representatives of p53 and p53-null cells. The role of the metal is relevant and it is likely that the metal-mediated oxidative stress plays an essential role in the whole process. The mechanisms induced by these molecules differ not only as a function of cell line but also of dose. The responses include two distinct self-destructive processes, autophagy and apoptosis.

Introduction

Thiosemicarbazones are a class of compounds widely investigated for their use as analytical reagents[1] and in the field of material science[2, 3], but most of all for their biological properties[4-9]. In this latter field, their activity stretches from antitumour[7] to antiviral[10, 11], from mycotoxigenic and antifungal[12, 13], to antimicrobial[14]. Among thiosemicarbazones, bisthiosemicarbazones are a subgroup of molecules with peculiar properties[9, 15] and have been recently investigated as potential nuclide carriers for medical imaging[16]. They present very interesting pharmacological properties often related to their ability to link metal ions more strongly than thiosemicarbazones by chelate effect, thanks to their higher denticity. Many bisthiosemicarbazone metal complexes have been studied as diagnostic and therapeutic radiopharmaceuticals[15], and the search for more effective thiosemicarbazone metal complexes is constantly progressing. One of their peculiarities is to allow a higher uptake in cells that grow in oxygen poor environments. The term "hypoxia" is generally used to describe low oxygen concentrations in a biological environment and this condition seems to have a deep impact on the development and subsequent treatment of a number of disease types, including cancer[16]. The low oxygen concentration usually corresponds to a poor vascularisation within a tumour mass, which in turn contributes to hinder the delivery of chemotherapeutic drugs to the target cells[16] and to render solid tumours more resistant to chemotherapy and radiotherapy treatments[17]. Patients with hypoxic tumours often present lower survival rates due to scarcely effective drug delivery. The mechanisms underlying the antitumor activity of thiosemicarbazone metal complexes[4] is not completely clear, and this is even more so for bis(thiosemicarbazonato) copper(II) complexes. It is reported, though, that small changes in the non-chelating part of the molecules produce dramatic changes in their physico-chemical properties, such as redox potentials and membrane permeability, and consequently in their overall biological activity[15]. In this paper, we report a comparative study between two bisthiosemicarbazones and their copper(II) complexes. Taking as starting molecules 2,3-butanedione-bis(4,4-dimethyl-3-thiosemi carbazone) and its copper complex, a compound already under study as a radiopharmaceutical[18, 19] and known to accumulate in cells in a hypoxic environment, we decided to explore its biological activity as a potential anticancer agent and to compare its behavior with that of 2,3-butanedione-bis(2-methyl-3-thiosemicarbazone) and its copper(II) complex. The peculiarity of this latter compound is that, since the ligand cannot deprotonate, the copper complex is cationic and, to our knowledge, no cationic bisthiosemicarbazone copper complex have been investigated so far for its biological properties, whereas only very recently the biological activity of copper cationic thiosemicarbazones has been reported with respect to neutral analogues[20]. To complete the study, we have carried out an extended biological study on a p53-null U937 leukemia and on an A549 adenocarcinoma cell line, cultured also under hypoxic conditions.

[a] Department of Chemistry, University of Parma, Parma, Italy. *E-mail: giorgio.pelosi@unipr.it; Fax: +39 0521905557; Tel: +39 0521905420
[b] Inter-University Consortium for Research on Chemistry of Metals in Biological Systems (C.I.R.C.M.S.B.), Parma Research Unit, 43124 Parma, Italy.
[c] Laboratory of Industrial Toxicology, Department of Clinical and Experimental Medicine, University of Parma, Parma, Italy
Electronic Supplementary Information (ESI) available. See DOI: 10.1039/x0xx00000x

The study includes cell viability, cell cycle, morphological changes, assessment of apoptosis, analysis of autophagy, measurement of reactive oxygen species (ROS) and of lipid peroxidation, protein determination, assessment of the expression of p53 and cellular uptake of metal complexes.

Experimental

Materials and techniques.

4,4-dimethyl-3-thiosemicarbazide, 2-methyl-3-thiosemicarbazide, 2,3-butanedione and copper(II) chloride were purchased from Sigma Aldrich. C, H, N, S analyses were obtained with a Carlo-Erba 1108 instrument. IR spectra were recorded using a Nicolet 5PC ATR-FTIR spectrophotometer, directly on the ATR accessory in the 4000-400 cm^{-1} range. The relative intensity of reported FT IR signals are defined as s = strong, br = broad, m = medium, and w = weak. ^1H NMR spectra were recorded on a Bruker Avance spectrometer at 300 MHz with TMS as the internal reference. The splitting of proton resonances in the reported ^1H NMR spectra are defined as s = singlet, br s = broad singlet, d = doublet, t = triplet, and m = multiplet. Electrothermal atomic absorption with Zeeman effect background correction (ETAAS) was conducted using a Perkin Elmer Pin AAcle 900Z Atomic Absorption Spectrometer (Waltham, MA, USA). Sterile plastic material for cell culture was purchased from Costar, Corning (Amsterdam, The Netherlands), RPMI 1640 medium, fetal bovine serum and phosphate buffered saline (PBS) from Euroclone (Milan, Italy). Annexin V/FITC kit Assay was obtained from Bender MedSystems GmbH (Vienna, Austria), Cyto-ID® Autophagy Detection kit from Enzo Life Sciences International Inc. (Plymouth Meeting, PA, USA), BCA Protein Assay from Thermo Scientific (Rockford, IL, USA), PerFix-nc Kit from Beckman Coulter, (Brea, CA, USA), caspase-8 and caspase-9 Fluorometric Assay kits from Biovision (Milpitas, CA, USA). DCFH-DA and EnzChek® caspase-3 assay kit were provided from Molecular Probes (Eugene, OR, USA). FITC mouse anti-human p53 were purchased from Dako Italia s.r.l. (Milan, Italy), along with their respective isotype controls. All other reagents were from Sigma (St. Louis, MO, USA), unless otherwise specified.

Syntheses of the ligands. 2,3-butanedione-bis(4,4-dimethyl-3-thiosemicarbazone) Me_2H_2But (1) (Fig. 1) was synthesized following a modified reported procedure[21]. The same procedure was followed also in the synthesis of 2,3-butanedione-bis(2-methyl-3-thiosemicarbazone) MeBut (2) (Fig. 2). Briefly, the proper thiosemicarbazide (4,4-dimethyl-3-thiosemicarbazide 0.206 g, 1.73 mmol, or 2-methyl-3-thiosemicarbazide 0.255 g, 2.43 mmol) was dissolved in 20 mL of ethanol 95% at reflux temperature under magnetic stirring. To the resulting solution was added a mixture of 2,3-butanedione (0.076 mL, 0.86 mmol, or 0.107 mL, 1.22 mmol respectively) dissolved in 10 mL of ethanol 95%. The resulting solution was kept stirred at reflux temperature for 6 h and during this time the colour turned from yellow to red. The reaction was monitored by TLC (hexane : ethyl acetate = 3 : 7). The solution was then transferred into a crystallizer and was allowed to evaporate at room temperature. The isolated red solid product was characterized by IR, NMR, Elemental Analysis and MS. Both ligands were isolated in good yields (85 % ca.).

Me_2H_2But (1). FT-IR: 3293 cm^{-1} NH (m), 2926 cm^{-1} CH (m), 1671 cm^{-1} C=N (s), 1536 cm^{-1} N-C=S (m), 927 cm^{-1} C=S (w).
NMR: (400MHz, DMSO D6) δ 1.96, 2.14, 2.33, 3.10 (3H each, s, CH_3-N); 3.33 (6H,s, CH_3-C=C), 9.54 (2H, s, NH).
ESI-MS: 289 MH^+.
E.A. % (exp): C 41.6 (41.15), H7.1 (7.06), N 29.1 (29.34), S 22.2 (23.17).

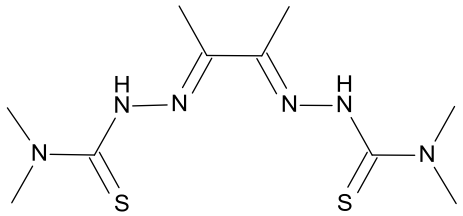

Fig. 1. Schematic view of compound Me_2H_2But (**1**).

MeBut (2). FT-IR: 3400, 3276 cm^{-1} NH_2(m), 2925 cm^{-1} CH (m), 1616 cm^{-1} C=N (s), 1571 cm^{-1} N-C=S (m), 935 cm^{-1} C=S (w).
NMR: (400MHz, DMSO D6) δ 3.42 (6H, s, CH_3-C=C), 3.93 (6H, s, CH_3-N), 7.31 (4H, bs, NH_2)
ESI-MS: 261 MH^+.
E.A. % (exp): C 36.9 (37.05), H 6.2 (6.23), N 32.3 (32.18), S 24.6 (24.55).

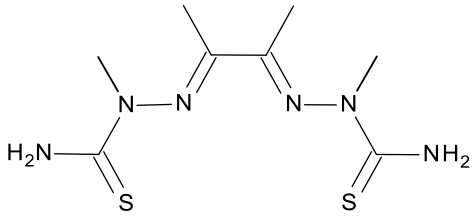

Fig. 2. Schematic view of compound MeBut (**2**).

Syntheses of the complexes.

[Cu(Me_2But)] (3). 2,3-butanedione-bis(4,4-dimethyl-3-thiosemi carbazone) Me_2H_2But (0.205 g, 0.71 mmol) was dissolved in 40 mL of ethanol 95% under stirring. Copper chloride in a 1:1 molar ratio with respect to the ligand (0.121 g, 0.71 mmol) was dissolved in 20 mL of ethanol 95% under stirring and was slowly added to the ligand solution. The resulting mixture was kept under stirring for 30 min and turned dark red-brown. It was then transferred to a crystallizer and left evaporating slowly at room temperature. The solid brown product isolated was recrystallized from a EtOH:H_2O 2:1 solution and characterized.
FT-IR: 2926 cm^{-1} CH (m), 1634 cm^{-1} C=N (s), 1526 cm^{-1} N-C=S (w).
ESI-MS: 351 MH^+.

E.A. % (exp): C 34.3 (34.29), H 5.2 (5.55), N 24.0 (24.14), S 18.3 (18.30).

[Cu(MeBut)]Cl_2(4). 2,3-butanedione-bis(2-methyl-3-thiosemicarbazone) MeBut (2) (0.139 g, 0.53 mmol) was dissolved in 50 mL of ethanol 95% under stirring. Copper chloride in a 1:1 molar ratio with respect to the ligand (0.017 g, 0.53 mmol) was dissolved in 20 mL of ethanol 95% under stirring and was slowly added to the ligand solution. The resulting mixture was kept under stirring for 1 hour at room temperature and turned dark red. Then it was transferred to a crystallizer and left evaporating slowly. A black powder was then isolated and characterized.
FT-IR: 3400, 3276 cm^{-1} NH_2(m), 2925 cm^{-1} CH (m), 1606 cm^{-1} C=N (s), 1565 cm^{-1} N-C=S (m), 927 cm^{-1} C=S (w).
ESI-MS: 325 MH^+-$2Cl^-$.
E.A. % (exp): C 24.3 (24.25), H 4.1 (4.19), N 21.3 (21.05), S 16.2 (16.68).

Cell lines. The A549 and U937 cells were purchased from the American Type Culture Collection (ATCC, Manassas, VA, USA). Cells were grown in RPMI 1640 medium containing 10% heat-inactivated fetal bovine serum, 100 U/mL penicillin and streptomycin at 37°C with 5% CO_2. Experiments were conducted with cells in the log phase and A549 adherent cell were the cells were harvested using trypsin.

Morphological observations. To observe the cell morphology, A549 cells were cultured and treated with compounds on glass slides. After 24 h exposure, the medium was removed, the specimens were fixed, stained with haematoxylin and eosin, and observed through a light microscope Olympus (Olympus, Tokyo, Japan).

Cell viability assay. Drug effects on cell viability were analyzed by 3-(4,5-dimethylthiazol-2-yl)-2,5-diphenyltetrazolium bromide (MTT) colorimetric assay, based upon the ability of metabolically active cells to reduce MTT into formazan by the action of mitochondrial dehydrogenases. A549 (70,000/ml) and U937 (150,000/ml) were seeded into 96-well plates overnight, and then exposed with compounds at indicated concentrations. At the end of treatment, MTT was added (final concentration 0.5 mg/ml) for 3 hours at 37°C and formazan crystals were dissolved in 100 µl for each well of acidic isopropanol (0.08 N HCl). After mixing, absorbance was evaluated by Multiskan Ascent microwell plate reader equipped with 550 nm filter (Thermo Labsystems, Helsinki, Finland). At least three independent experiments were performed with eight replicate wells per sample. The half maximal inhibitory concentration (IC_{50}) was determined as the concentration resulting in 50% cell growth reduction compared with untreated control cells.

Cell cycle. Flow cytometry was used to evaluate the cell phase distribution by determining the nuclear DNA content, as already described [22]. Briefly, cells were collected, washed in PBS, and fixed in ethanol (96%) before staining by propidium iodide (PI- 20 µg/mL in PBS containing RNase-A). Cells were sorted in a FC500™ flow cytometer (Beckman Coulter, Brea, CA, USA), and percentages of cellular phases were calculated by FlowJo software (Ashland, OR, USA).

Assessment of apoptosis. Apoptosis in both A549 and U937 cells was evaluated by using the Annexin V-Propidium Iodide (PI) method. Briefly, cells exposed to different concentrations of compounds for 24h, were washed in PBS, incubated with Annexin V-FITC and propidium iodide (PI) at room temperature for 15 min in the dark and analyzed by FC500™ flow cytometer (Instrumentation Laboratory, Bedford, MA, USA). The data analysis was performed using FlowJo software (Tree Star Inc.). Apoptosis was calculated as percentage of early and late apoptotic cells. Apoptosis analysis was completed by the quantification of caspases activity using fluorometric assay kits, according to the manufacturers' protocols. Cell lysates were incubated in the reaction buffer with the corresponding substrates: Ile-Glu-Thr-Asp (IETD)-AFC (7-amino-4-trifluoromethyl coumarin) for caspase-8, Leu-Glu-His-Asp (LEHD)-AFC for caspase-9 and rhodamine 110 bis-(N-CBZ-L-aspartyl-L-glutamyl-L-valyl-L-aspartic acid amide) (Z-DEVD-R110) for caspase-3. Enzymatic cleavage of the substrates produced fluorescent probes, which were quantified by a Cary Eclipse fluorescence spectrophotometer (Varian, Inc., Palo Alto, CA, USA). Enzymatic activity was referred to the protein content and expressed as percentage of unexposed control.

Analysis of autophagy. Autophagic activity at cellular level was assessed by flow cytometry and fluorescence microscopy using a commercial assay, according to the producer's procedures.
To quantitative analyze autophagy, the cells were treated with compounds in presence or absence of 3-methyladenine (3MA) (10 mM). After 24 h of treatment, the cells were collected, washed with PBS and subsequently incubated for 30 min at 37˚C in the dark with the Cyto-ID Green Detection Reagent, diluted in culture medium without phenol red indicator and supplemented with 5% FBS. The probe was then removed by centrifugation and wash with PBS were added and resuspended cells were immediately analyzed by FC500™ flow cytometer (Beckman Coulter, Brea, CA, USA) Analysis was performed using FlowJo software (Ashland, OR, USA). Flow cytometry allowed the monitoring of changes in cellular physical parameter (SSC and FSC).

To visualize autophagic vacuoles lung cancer adherent cells were stained with the same specific autophagosome marker. Briefly, A549 were seeded and cultured on microscopy slides to approximately 70% confluence, before treatment with complexes at indicated concentrations. Untreated cells were used as negative control. After 24 hours cells were carefully washed, because autophagic cells tend to get loose and can be easily dislodged from the slides and tend to get loose. The dye diluted in assay buffer containing FBS 5% was applied to the slides for 30 minutes at 37°C, then the cells were washed and fixed with 4% paraformaldehyde for 20 minutes before the nuclear staining with DRAQ5® (Cell Signaling Technology, Danvers, MA, USA).

Sample were observed using a confocal system (LSM 510 Meta scan head integrated with the Axiovert 200 M inverted microscope Carl Zeiss, Jena Germany) with a 63x/1.30 oil objective.

Image acquisition was carried out in multitrack mode, namely through consecutive and independent optical pathways.

Oxidative stress. The effects of compounds tested on intracellular redox equilibrium were assessed by the measurement of reactive oxygen species (ROS) and of lipid peroxidation[22]. The generation of ROS in the cells following treatment was determined using 2,7-dichlorodihydrofluorescein diacetate (H2-DCFDA). The process involves elimination of the acetate groups (non-fluorescent) by intracellular esterases, DCFH can react with intracellular ROS to form the highly fluorescent 2',7'-dichlorofluorescein (DCF). The cells were pretreated for 30 minutes with H2-DCFDA (working concentration 10 µM) and rinsed with PBS before the brief incubation (30-60 minutes) with tested compounds. After washing with PBS the fluorescent cells were evaluated by FC500™ flow cytometer (Beckman Coulter, Brea, CA, USA) Analysis was performed using FlowJo software (Ashland, OR, USA). ''Thiobarbituric Acid Reactive Substances'' (TBARS) method is the validated assay chosen to evaluate lipid peroxidation: malondialdehyde (MDA) derived from polyunsaturated fatty acids condenses with two equivalents of thiobarbituric and the fluorescent product can be quantitatively evaluated by a Cary Eclipse fluorescence spectrophotometer (Varian, Inc., Palo Alto, CA, USA) (excitation 515 nm, emission 545 nm). The values were normalized for the protein concentrations.

Protein determination. The BCA (bicinchoninic acid) Protein Assay (Thermo Scientific, Rockford, IL, USA) was used for the colorimetric determination of protein concentration, according to the manufacturer's instructions. A standard curve of serial concentrations of bovine serum albumin was generated to cover the full assay range (0-200 µg/ml).

Hypoxic treatments. During hypoxic experiments A549 cells were grown for 24 hours in Anaerocult C® mini system or in Anaerobic Jar (Merck Millipore, Darmstadt, Germany) in which a hypoxic environment (oxygen concentration less than 7%) was produced. Hypoxia was confirmed by the color change of the Anaerotest® strip indicator (Merck Millipore, Darmstadt, Germany) located in the bag or jar.

P53 analysis. Expression of p53 was assessed by using specific FITC-labeled mouse monoclonal antibody anti-human p53. Adherent cells were fixed and permeabilized with Per-Fix Kit according to manufacter's, and incubated with the fluorescent antibodies for 30 minutes in the dark before flow cytometry analysis (FC500™ flow cytometer, Beckman Coulter, Brea, CA, USA). Isotype controls were included.

Statistical analysis. Data were analysed using GraphPad Prism v5 (GraphPad Inc., San Diego, CA, USA). The results are presented as the mean ± standard deviation of at least three independent experiments. The statistical analyses were carried out using one-way ANOVA, followed by Dunnett's or Turkey's post hoc tests. p values < 0.05 were considered as significant.

Copper uptake. Intracellular Cu concentrations were determined over a 24 hour period of treatment in cell lines U937 and A549. Briefly, the cell pellets were collected, re-suspended in 100 ml of water, freeze/thawed three times, and centrifuged (1200g for 5 min). The supernatant was analysed by means of electrothermal atomic absorption with Zeeman effect background correction (ETAAS), using a Perkin Elmer Pin AAcle 900Z Atomic Absorption Spectrometer (Waltham, MA, USA). Certified standards were directly prepared in the supernatant of unexposed cells in order to reduce the matrix effect. The limit of detection (LOD), calculated as 3SD of the blank, was 0.5 mg/ l.Cu concentrations were normalized for cell count and expressed as ng/10^6 cells.

Results and discussion

Comparing the IR spectrum of ligand (**1**) with that of its metal complex (**3**), it is apparent that deprotonation occurs upon coordination, and this confirms the neutral molecular nature of the copper complex.

In the spectra of the complexes, the C=N, C=S and N=C=S stretchings are shifted at lower wavenumbers with respect to the signals of the same functional groups in the spectra of the ligands, confirming the N,S,S,N coordination around the metal ion for both complexes (**3**) and (**4**).

The octanol-water distribution coefficient, logD at pH 7.40 was calculated[23] for both ligands and it was found to be 1.25 for Me_2H_2But (**1**) and 0.80 for MeBut (**2**). The octanol-water partition coefficient, logP were also calculated[24] for Me_2H_2But (**1**): 2.13, MeBut (**2**): 0.60; [Cu(Me_2But)] (**3**): 1.76 and [Cu(MeBut)]Cl_2(**4**): -4.74. Passing from Me_2H_2But (**1**) to MeBut (**2**), there is an increase of the molecule concentration in the aqueous phase and a further increase takes place upon complexation, reaching its apex with the ionizable compound [Cu(MeBut)]Cl_2 (**4**).

The ligand Me_2H_2But (**1**) is inactive on cell line A549 and moderately active on cell line U937 (Table 1). The corresponding copper complex results to be more potent than the ligand: its IC_{50} is about 10-fold lower in cell line U937. The IC_{50} values also demonstrate that U937 cells are more sensitive than the lung derived solid tumor A549. Both cell lines exhibit an analogous behaviour when treated with MeBut (**2**) and [Cu(MeBut)]Cl_2 (**4**): the ligand does not affect cell viability at any of the tested concentrations, while the IC_{50}'s of the complex, determined after 24h treatment, are almost the same in both cell lines.

As a control, both cell lines were also exposed to the inorganic salt at concentrations up to 20 µM without observing any significant effect on cell proliferation. The findings are consistent with the analysis of the cell cycle progression which is slightly perturbed by ligand Me_2H_2But (**1**) only in U937 and more markedly altered by the copper complexes in both cell lines, resulting in inhibition of proliferation (Fig. 3). The number of A549 cells accumulated in G2/M increased over a 24 hour treatment. In U937 cultures, all stages are remarkably altered

and a significant sub-G0/G1 peak is observed, revealing DNA fragmentation, absent in A549 and suggesting the upsurge of apoptosis.

The cytogram distribution of Cu complexes-treated A549 (Fig. 4) shows an increased side scatter (SSC) (59,1+5,32% for [Cu(Me_2But)] (**3**) and 43,87+6,11% for [Cu(MeBut)]Cl_2(**4**) after 24h). These changes in SSC distribution are clearly evident already at an early stage, suggesting changes of internal structure and of the number and type of organelles present in the cell. All these details are frequently related to autophagy.[25]

	IC_{50} (μM) (24 h)	
	U937	A549
Me_2H_2But (**1**)	21.10±2.99	>100
[Cu(Me_2But)] (**3**)	2.53±0.81	7.52±2.13
MeBut (**2**)	>100	>100
[Cu(MeBut)]Cl_2(**4**)	8.90±1.22	9.58±0.64

Table 1. IC_{50} values of ligands and Cu complexes for the A549 and U937 cell lines. Results are shown as means ± SD

These observations led us to analyse the apoptotic and autophagic pathways. In order to determine whether these effects were associated with apoptosis, phosphatidylserine translocation and caspase-3 activation were evaluated after 24 hours of exposure.

Treatment with the IC_{50} concentration of ligand (**1**) and of the complexes resulted in a significant increase, compared to controls, in apoptotic U937 cells, while in A549 no differences were observed (Fig. 5).

To characterize the pathway through which the complexes induce apoptosis, caspase-8 and caspase-9 activity was assessed after 8 hours. All three compounds that induce apoptosis in cell line U937, but to a different extent. The phenomenon is very limited with ligand Me_2H_2But (**1**) and much more intense in the presence complexes (**3**) and (**4**). Compound (**3**) triggers the activation of caspase-9, while compound (**4**) activates all the three caspases assayed, with a prevalence of caspase-9 (Fig. 6).

From the autophagy analysis, opposite results were obtained (Fig. 7): no evidence of autophagic activity was detected in U937 cells. In A549 cultures the copper complexes caused a significant increases of autophagosomes, as assessed by flow cytometry (increases of median fluorescence compared to controls: 67,2+4,74% for [Cu(Me_2But)] (**3**) and 35,25+4,51% for [Cu(MeBut)]Cl_2(**4**)) and by microscopy observations: autophagosomes, the morphological characteristics of autophagy, were observed to a greater extent in cells exposed to the lowest concentrations tested (Fig. 8A and 8B).

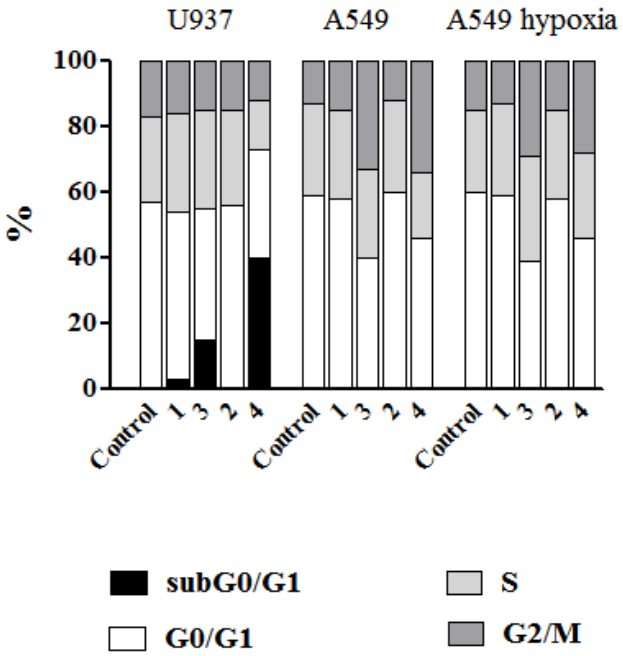

Fig. 3 Cell cycle distribution of cells treated with IC_{50} concentrations of ligands and Cu complexes. Monoparametric DNA analysis separate cells into three distinct phases, corresponding to different peaks: G0/G1, S and, G2/M phase. Means of three different experiments

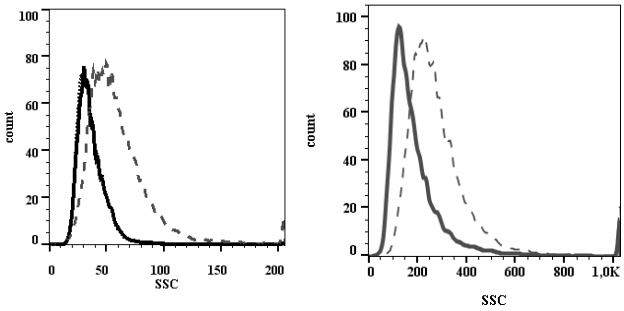

Fig. 4. Flow-cytometry analysis of side scatter (SSC) in A549 cells for compounds **3** (left) and **4** (right). Unexposed cells were scanned as control (continuous line) and compared to cells exposed to IC_{50} for 24h (dashed line).

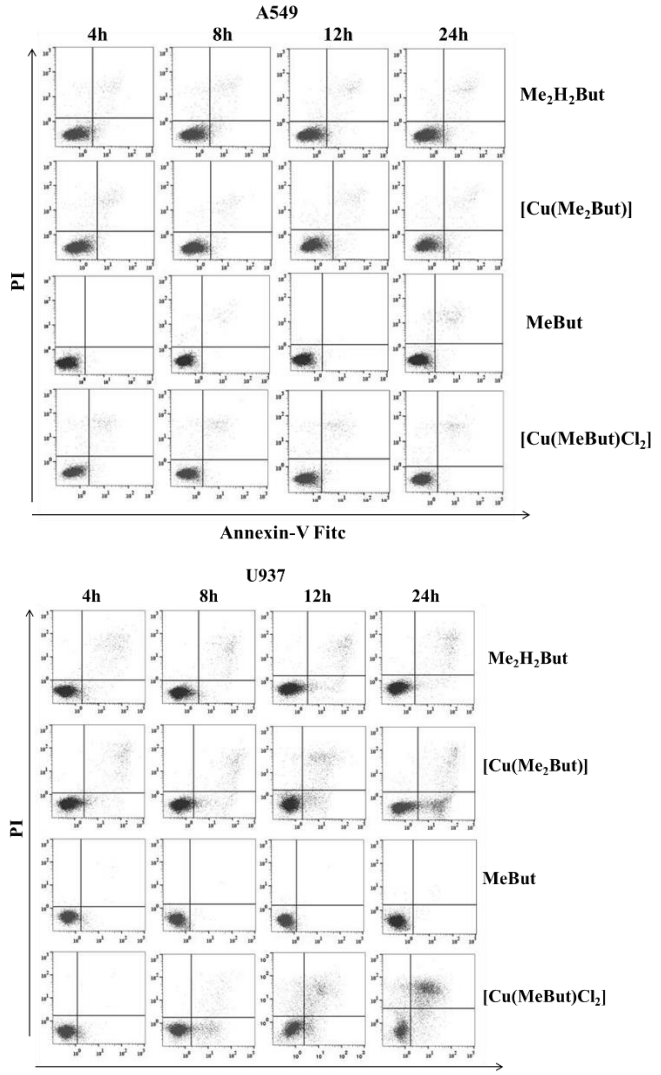

Fig. 5. Flow cytometry analysis of apoptosis after cell staining with annexin V-FITC/PI. Annexin V-FITC(+)/PI(-) cells were considered early apoptotic and Annexin V-FITC(+)/PI(+) cells were considered advanced apoptotic or necrotic.

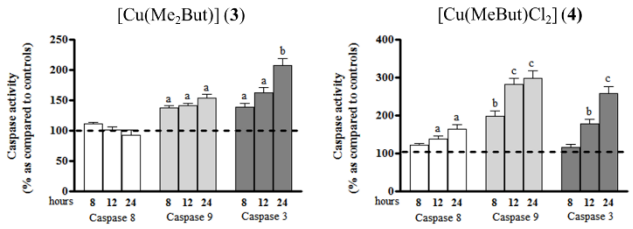

Fig. 6. Caspase-3, -8 and -9 activities were evaluated in U937 cultures during exposure to IC_{50} concentrations of Cu complexes. Results (mean +SD of three separate experiments carried out in triplicate) are expressed as percentage vs control = (sample value/control value) x 100. Significantly different from untreated control: [a]: $p < 0.05$; [b]: $p < 0.01$, [c]: $p < 0.001$.

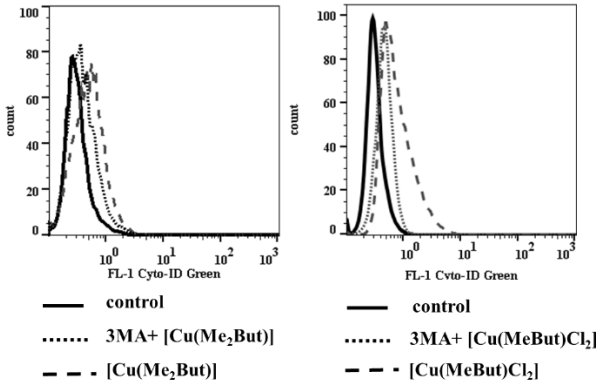

Fig. 7. Flow cytometry-based analysis of autophagy induction in A549 cells treated with Cu complexes for 24 h. Results are presented as histogram overlay. (Control: solid line; Cu Complex treated cells: dashed line; Cu Complex +3MA treated cells: dotted line).

3-Methyl adenine (3MA), an inhibitor of type III phosphatidylinositol 3-kinases (PI-K3), completely blocked these self-degradative processes and reduced SSC. This assay confirms the nature of phenomenon (Fig. 7).

The levels of p53 protein in A549 cultures along the time course of treatment (24h) were determined by flow cytometry. The protein expression increased in the presence of the Cu complexes, peaking at 4–8 h and declining at 24 h post-treatment (Fig. 9).

Intracellular ROS were then assayed. MeBut (**2**) did not cause oxidative stress, while Me_2H_2But (**1**) and the two complexes induced in both cell lines intracellular ROS production. Only after exposure to [$Cu(Me_2But)$] (**3**), ROS generation was associated/coupled with lipid peroxidation (TBARS). [$Cu(MeBut)Cl_2$] (**4**) enhanced TBARS levels only in U937 cells, but not in the lung line (Fig.10).

The compounds were also tested to study the influence of lower oxygen levels in the solid tumour cell line A549. The IC_{50} of complexes under hypoxia was about 2 and 2.5-fold higher for compounds (**3**) and (**4**) as compared to that under normoxia (Table 2).

IC_{50} (μM) (24 h) for A549		
	normoxia	hypoxia
Me_2H_2But (**1**)	>100	>100
[$Cu(Me_2But)$] (**3**)	7.52±2.13	14.09±3.29
MeBut (**2**)	>100	>100
[$Cu(MeBut)Cl_2$] (**4**)	9.58±0.64	23.09±1.54

Table 2. Comparison of the IC_{50} values in normoxia and hypoxia for the four compounds on cell line A549

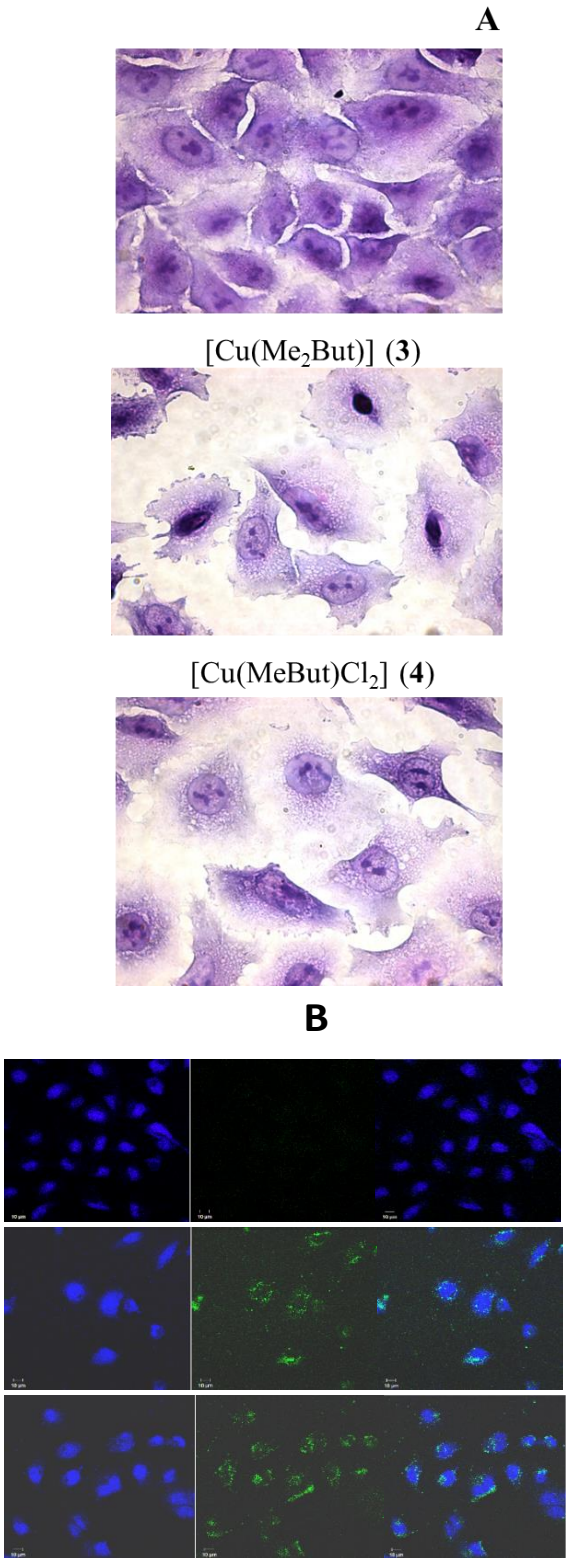

Fig. 8. Morphological phenomena of autophagy in complex-treated lung cancer cells (5 µM for 24h). (A) Direct observation under a light microscope of hematoxylin-eosin stained cells (Magnification, x200). B) Samples stained with autophagy probe were examined under confocal microscope. First row: control; middle row: [Cu(Me_2But)] (**3**); third row: [Cu(MeBut)]Cl_2 (**4**).

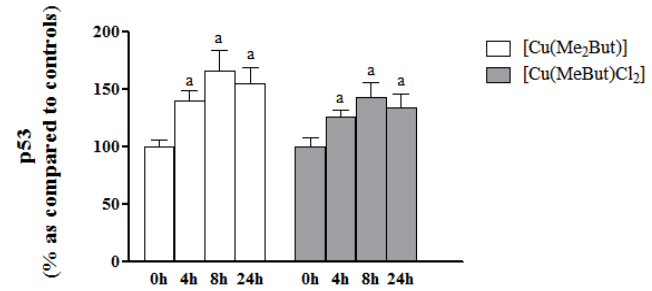

Fig. 9. Influence of the incubation time on p53 expression in A549 cells treated with Cu Complexes. Data are expressed as Mean (treated/control) ± SD. Significantly different from untreated control: [a]: $p < 0.05$.

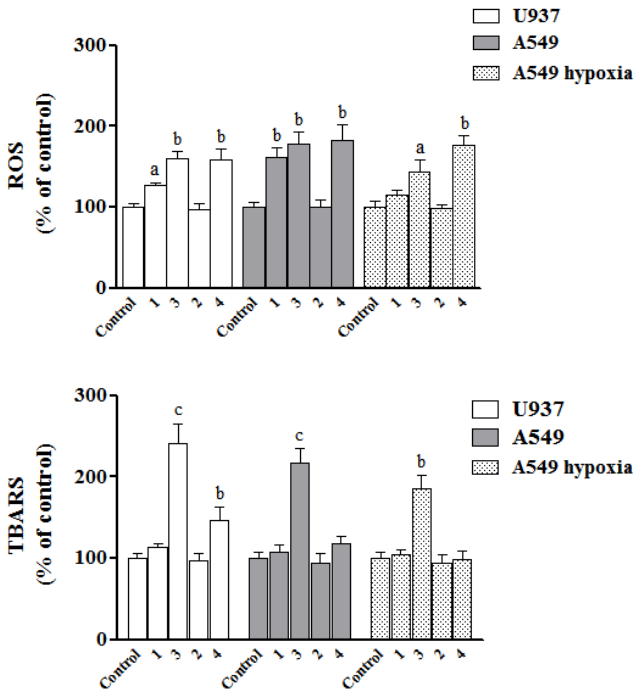

Fig. 10. ROS production (above) during cells exposure to IC_{50} concentrations and lipid peroxidation (below): TBARS production after 24h treatment with IC_{50} concentrations. Values are mean ± SD of three separate experiments, each carried out in triplicate and expressed as percentage of control. Significantly different from untreated control: [a]: $p < 0.05$; [b]: $p < 0.01$; [c]: $p < 0.001$.

It is noteworthy that the modification of the cell cycle is independent by the levels of available oxygen, while hypoxia caused a significant reduction of reactive oxygen species for (**1**) and (**3**). Moreover hypoxia significantly augmented (**4**)-induced autophagy activation, while during treatment with (**3**) the oxygen concentrations did not affect the autophagic processes.

To evaluate the metal content, cells were exposed at metal

complex concentrations as low as 1 μM to avoid cellular damages. The intracellular Cu concentrations in A549 and U937 over 24 hours are reported in Fig. 11. From the curves it is apparent that complexes easily enter both cell lines and that uptake increases during the 24 hours with similar rates.

It is also worthy of note the different metal uptake shown for the two complexes (Fig. 11). The complex [Cu(MeBut)]Cl_2 (**4**) is absorbed 4 times more than [Cu(Me_2But)] (**3**) by cell line U937 and 5 times more by cell line A549. In addition, the uptake is larger in the solid tumour than in the leukemic one.

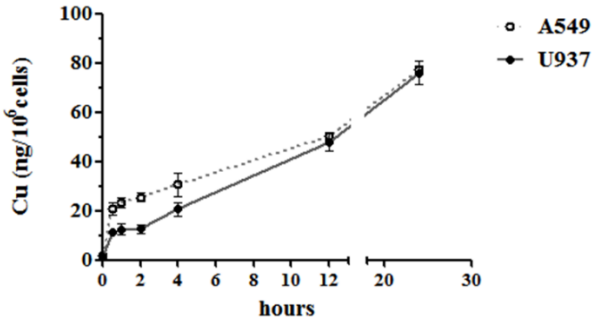

[Cu(Me_2But)] (**3**)

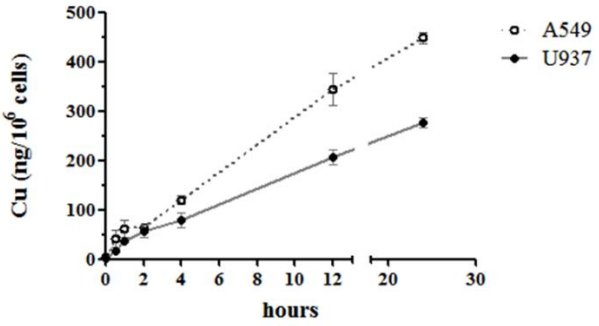

[Cu(MeBut)]Cl_2(**4**)

Fig. 11. Evaluation of Cu uptake in A549 and U937 cells treated with complexes. Intracellular metal was measured over a 24 hour period. Results are shown as means SD.

A possible interpretation of this phenomenon is that complex (**4**) behaves as cisplatin, being neutral in the culture medium, where the chloride concentration is of the order of magnitude of 10^{-1}M, and becoming cationic once in the cytoplasm, where the concentration of chloride ions drops to 10^{-3}M. As can be noticed from the uptake diagrams, in the first 2 hrs the copper uptake rate is very similar for both complexes and both cell lines. With time, complex (**3**) absorption increases at a slow rate, while the uptake of compound (**4**) increases rapidly and this may be due to a partial/total dissociation of [Cu(MeBut)]Cl_2 to $[Cu(MeBut)Cl]^+$ and $[Cu(MeBut)]^{2+}$ species which, being charged, cannot diffuse across the cell membrane. Nevertheless, the high increase of copper(II) uptake with time in cell line A549 (see Fig 9) suggests also the presence of some sort of active uptake mechanism which must be absent in cell line U937.

Conclusions

The four compounds under study elicit different effects on the two lines adopted as representatives of p53 (A549) and p53-null (U937) cells. The role of the metal is of great relevance and it is likely that the metal-mediated oxidative stress plays an essential role in the whole process. The responses include two distinct self-destructive processes, autophagy (or self-eating) and apoptosis (or self-killing), involved in the turnover of cytoplasmic organelles or whole cells, respectively.

As a general trend, from our data, we can notice that the two metal complexes, even though at different levels, induce ROS production, but while in p53 null cells the response is directly apoptosis, in cell line A549, probably due to the mediation of p53, an autophagic response that somehow prevents the onset of apoptosis is triggered. Something similar, but at a very low level, can be said for ligand **1** and its behaviour might be associated to its capability to undergo a thione-thiol tautomerism, a process hampered，in ligand **2**， by the methyl groups in place of the acidic H. The presence of these oxidizable sulfide groups could be involved in redox processes and ROS production.

Nevertheless, much caution is needed because, although autophagy and apoptosis are under the control of multiple common upstream signals, autophagy-apoptosis cross-talk seems to be very complex [25]. Some adverse conditions elicit autophagy and apoptosis within the same cell, mostly in a sequence in which autophagy precedes apoptosis. This is because stress often stimulates an autophagic response, especially if damage is not lethal. Apoptotic or non-apoptotic lethal processes are activated when stress exceeds a critical threshold of intensity or lasting. However, in the majority of cases, apoptosis and autophagy seem to cross-regulate each other, mostly in an inhibitory manner: autophagy reduces the propensity of cells to undergo apoptosis, and caspase activation shuts off the autophagic process. In our study, the mutually inhibitory control of these processes are evident: while apoptosis is the main response in U937, the treatment of A549 cells with the complexes induces autophagic activity.

The different effects produced and the observed susceptibility might depend on the peculiarities of the cancer lines that have been tested: U937 cells are functionally p53 null as a consequence of a large deletion in the p53 gene[26], while A549 are p53 wild-type[27]. p53 is the most commonly mutated gene in tumours. It is considered the 'guardian of the cellular genome' because in response to DNA damage, oncogenic activation, hypoxia or other stress, this protein can activate and coordinate cellular responses, either to prevent and repair genetic damage or to eliminate potentially oncogenic cells.

Increasing evidence suggests that this protein is not only involved in control of cell-cycle arrest and cell death, but represents a central node in response networks and regulates cellular autophagy[28]. It acts in a two-faced fashion[29]: the p53 tumour suppressor was thought to positively regulate autophagy, but now we know that it may also inhibit it. However, when cells are subjected to oncogenic activation or genotoxic stress and p53 is activated, stimulation of autophagy occurs. Thus, p53 is considered a positive regulator of autophagy and its activation might suggest that it is part of the protective function of p53 [30]. In agreement with this hypothesis, in this study autophagy was induced in the p53 wild-type cell line A549 but not in mutant-type cells U937. These results suggest that p53 plays a dramatic role in inducing autophagy and in inhibiting apoptosis during the treatment with the metal complexes. This dramatic role is highlighted by the fact that even though these A549 cells absorb much larger amounts of copper(II) than their counterpart (p53-null cell line U937) they do not undergo apoptosis. Similar autophagic processes induced by cisplatin in lung cancer cells have been reported in recent studies[31, 32]. Cho also evidenced the role of p53: the induction of autophagy by low-dose cisplatin was increased by 2-fold in wild-type p53 cells compared to the null-type p53 ones. It was also hypothesized that autophagy contributes to the development of cisplatin resistance in human lung adenocarcinomas, thus playing a survival role in protecting cells from cisplatin-mediated cytotoxicity. Besides the function of autophagy in cisplatin, treatment is still controversial; the authors speculate that autophagy can be used as a novel therapeutic target to overcome cisplatin-resistant lung adenocarcinoma.

The higher IC_{50}'s under hypoxia, as compared to those under normoxia, confirm that this condition significantly increase cell viability upon treatment with both complexes, suggesting that hypoxia, to some extent, protects cells from induced cell death. It was generally acknowledged that in hypoxic condition cancer cells undergo metabolic and genetic changes, mediated by hypoxia-inducible factor (HIF-1α), that allow them to be more resistant to chemotherapics[33-37]. Similar results were obtained in cisplatin-treated A549 cells[38]. These authors show that hypoxia robustly augmented cisplatin-induced autophagic process and markedly reduce apoptosis. They conclude that under normoxia, autophagy activation is unable to counteract the stress induced by cisplatin, therefore resulting in cell death, whereas under hypoxia, the increased autophagic induction removes this stress, allowing the cells to survive and decreasing lung-cancer cell susceptibility to cisplatin-induced apoptosis. Nevertheless, the role of hypoxia in cell death or survival is still not elucidated[33, 39]. The contradictory conclusions reported might reflect the differences in defining 'hypoxia'. When autophagy is induced under conditions of well-controlled hypoxia with no nutrient limitation and appropriate pH control, it has pro-survival effects, while autophagy induced under severe hypoxia and concomitant to metabolic stress, it is often associated with cell death. In solid tumours hypoxic gradients are highly dynamic and in the same tumor both responses might be present[39].

Our complexes did not trigger apoptosis in A549 cultures under any oxygen concentration. Hypoxia increased the autophagic process only in A549 cells exposed to (**4**), but did not significantly change cellular response to (**3**) probably because it was already close to the maximum detectable levels.

Hypoxia did not suppress ROS production induced by the complexes, particularly for (**4**). The idea that hypoxic conditions reduce oxidative stress due to limiting oxygen levels is in contrast with the observation that the levels of intracellular ROS, paradoxically, can increase under hypoxia. The precise mechanism is not yet clarified, but it seems that ROS production is due to the absence of the final electron acceptor (O_2) on the mitochondria electron transport chain[40].

More work is in development to explore the role that copper chaperones expression in these two cell lines might have in the different response to the copper complexes used in these experiments. [41]

Acknowledgements

Mr Giacomo Ganazzoli and Ms Federica Curti are acknowledged for their technical support. The authors thank the University of Parma for the financial support and the Centro Interdipartimentale Misure (C.I.M.) for the use of NMR facilities.

References

1 S. A. Reddy, P. V. Raman and A. V. Reddy, Synthesis of novel analytical reagent, 2,6-diacetylpyridine bis-4-phenyl-3-thiosemicarbazone and its analytical applications: Determination of Pd(II) in spiked samples, *Journal of Chemical and Pharmaceutical Research*, 2015, **7**, 146-154.

2 F. Bisceglie, G. Del Monte, P. Tarasconi and G. Pelosi, Synthesis and characterization of 4-fluorobenzaldehyde thiosemicarbazone derivatives as corrosion inhibitors, *Inorg Chim Acta*, 2015, **434**, 143-149.

3 D. D. N. Singh, M. M. Singh, R. S. Chaudhary and C. V. Agarwal, Inhibitive effects of isatin, thiosemicarbazide and isatin-3-(3-thiosemicarbazone) on the corrosion of aluminium alloys in nitric acid, *Journal of Applied Electrochemistry*, 1980, **10**, 587-592.

4 G. Pelosi, Thiosemicarbazone Metal Complexes: From Structure to Activity, *The Open Crystallography Journal*, 2010, **3**, 16-28.

5 H. Beraldo and D. Gambino, The wide pharmacological versatility of semicarbazones, thiosemicarbazones and their metal complexes, *Mini-Rev Med Chem*, 2004, **4**, 31-39.

6 F. Bisceglie, A. Musiari, S. Pinelli, R. Alinovi, I. Menozzi, E. Polverini, P. Tarasconi, M. Tavone and G. Pelosi, Quinoline-2-carboxaldehyde thiosemicarbazones and their Cu(II) and Ni(II) complexes as topoisomerase IIa inhibitors, *J Inorg Biochem*, 2015, **152**, 10-19.

7 D. S. Kalinowski, P. Quach and D. R. Richardson, Thiosemicarbazones: the new wave in cancer treatment, *Future Med Chem*, 2009, **1**, 1143-1151.

8 J. T. Wilson, X. H. Jiang, B. C. McGill, E. C. Lisic and J. E. Deweese, Examination of the Impact of Copper(II) alpha-(N)-Heterocyclic Thiosemicarbaione Complexes on DNA Topoisomerase II alpha, *Chem Res Toxicol*, 2016, **29**, 649-658.

9 P. A. Barrett, E. Beveridge, P. L. Bradley, C. G. D. Brown, S. R. M. Bushby, M. L. Clarke, R. A. Neal, R. Smith and J. K. H. Wilde, Biological Activities of Some alpha-Dithiosemicarbazones, *Nature*, 1965, **206**, 1340-1341.

10 D. Rogolino, A. Bacchi, L. De Luca, G. Rispoli, M. Sechi, A. Stevaert, L. Naesens and M. Carcelli, Investigation of the salicylaldehyde thiosemicarbazone scaffold for inhibition of influenza virus PA endonuclease, *J Biol Inorg Chem*, 2015, **20**, 1109-1121.

11 G. Pelosi, F. Bisceglie, F. Bignami, P. Ronzi, P. Schiavone, M. C. Re, C. Casoli and E. Pilotti, Antiretroviral Activity of Thiosemicarbazone Metal Complexes, *J Med Chem*, 2010, **53**, 8765-8769.

12 F. Degola, C. Morcia, F. Bisceglie, F. Mussi, G. Tumino, R. Ghizzoni, G. Pelosi, V. Terzi, A. Buschini, F. M. Restivo and T. Lodi, In vitro evaluation of the activity of thiosemicarbazone derivatives against mycotoxigenic fungi affecting cereals, *Int J Food Microbiol*, 2015, **200**, 104-111.

13 D. Secci, S. Carradori, B. Bizzarri, P. Chimenti, C. De Monte, A. Mollica, D. Rivanera, A. Zicari, E. Mari, G. Zengin and A. Aktumsek, Novel 1,3-thiazolidin-4-one derivatives as promising anti-Candida agents endowed with anti-oxidant and chelating properties, *Eur J Med Chem*, 2016, **117**, 144-156.

14 J. A. Lessa, M. A. Soares, R. G. dos Santos, I. C. Mendes, L. B. Salum, H. N. Daghestani, A. D. Andricopulo, B. W. Day, A. Vogt and H. Beraldo, Gallium(III) complexes with 2-acetylpyridine-derived thiosemicarbazones: antimicrobial and cytotoxic effects and investigation on the interactions with tubulin, *Biometals*, 2013, **26**, 151-165.

15 B. M. Paterson and P. S. Donnelly, Copper complexes of bis(thiosemicarbazones): from chemotherapeutics to diagnostic and therapeutic radiopharmaceuticals, *Chem Soc Rev*, 2011, **40**, 3005-3018.

16 I. S. Alam, R. L. Arrowsmith, F. Cortezon-Tamarit, F. Twyman, G. Kociok-Kohn, S. W. Botchway, J. R. Dilworth, L. Carroll, E. O. Aboagye and S. I. Pascu, Microwave gallium-68 radiochemistry for kinetically stable bis(thiosemicarbazone) complexes: structural investigations and cellular uptake under hypoxia, *Dalton T*, 2016, **45**, 144-155.

17 W. R. Wilson and M. P. Hay, Targeting hypoxia in cancer therapy, *Nat Rev Cancer*, 2011, **11**, 393-410.

18 R. A. Medina, E. Mariotti, D. Pavlovic, K. P. Shaw, T. R. Eykyn, P. J. Blower and R. Southworth, Cu-64-CTS: A Promising Radiopharmaceutical for the Identification of Low-Grade Cardiac Hypoxia by PET, *J Nucl Med*, 2015, **56**, 921-926.

19 P. J. Blower, T. C. Castle, A. R. Cowley, J. R. Dilworth, P. S. Donnelly, E. Labisbal, F. E. Sowrey, S. J. Teat and M. J. Went, Structural trends in copper(II) bis(thiosemicarbazone) radiopharmaceuticals, *Dalton T*, 2003, 4416-4425.

20 M. M. Subarkhan, R. N. Prabhu, R. R. Kumar and R. Ramesh, Antiproliferative activity of cationic and neutral thiosemicarbazone copper(II) complexes, *Rsc Adv*, 2016, **6**, 25082-25093.

21 D. X. West, J. S. Ives, G. A. Bain, A. E. Liberta, J. ValdesMartinez, K. H. Ebert and S. HernandezOrtega, Copper(II) and nickel(II) complexes of 2,3-butanedione bis(N(3)-substituted thiosemicarbazones), *Polyhedron*, 1997, **16**, 1895-1905.

22 R. Alinovi, M. Goldoni, S. Pinelli, M. Campanini, I. Aliat, D. Bersani, P. P. Lottici, S. Iavicoli, M. Petyx, P. Mozzoni and A. Mutti, Oxidative and pro-inflammatory effects of cobalt and titanium oxide nanoparticles on aortic and venous endothelial cells, *Toxicol in Vitro*, 2015, **29**, 426-437.

23 Marvin 6.3.0, 2014, ChemAxon (http://www.chemaxon.com).

24 MDL.Draw.Editor 16.1.0.693, 2016, Accelerys (http://www.accelerys.com).

25 (a) N. Mizushima, B. Levine, A.M. Cuervo and D.J. Klionsky, Autophagy fights disease through cellular self-digestion, *Nature*, 2008, **451(7182)**, 1069-1075. (b) S. Chatterjee, S.Sarkar and S. Bhattacharya, Toxic metals and Autophagy, *Chem. Res. Toxicol.*, 2014, **27**, 1887-1900. (c) K.M. Ryan, p53 and autophagy in cancer: Guardian of the genome meets guardians of the proteome, *Eur. J. Cancer*, 2011, **47**, 44-50. (d) G. Marino, M. Niso-Santano, E. H. Baehrecke and G. Kroemer, Self-consumption: the interplay of autophagy and apoptosis, *Nat Rev Mol Cell Bio*, 2014, **15**, 81-94.

26 K. Sugimoto, H. Toyoshima, R. Sakai, K. Miyagawa, K. Hagiwara, F. Ishikawa, F. Takaku, Y. Yazaki and H. Hirai, Frequent Mutations in the P53 Gene in Human Myeloid-Leukemia Cell-Lines, *Blood*, 1992, **79**, 2378-2383.

27 L. Q. Jia, M. Osada, C. Ishioka, M. Gamo, S. Ikawa, T. Suzuki, H. Shimodaira, T. Niitani, T. Kudo, M. Akiyama, N. Kimura, M. Matsuo, H. Mizusawa, N. Tanaka, H. Koyama, M. Namba, R. Kanamaru and T. Kuroki, Screening the p53 status of human cell lines using a yeast functional assay, *Mol Carcinogen*, 1997, **19**, 243-253.

28 K. M. Ryan, p53 and autophagy in cancer: Guardian of the genome meets guardian of the proteome, *Eur J Cancer*, 2011, **47**, 44-50.

29 B. Levine and J. Abrams, p53: The Janus of autophagy?, *Nat Cell Biol*, 2008, **10**, 637-639.

30 E. White, Autophagy and p53, *Csh Perspect Med*, 2016, **6**.

31 K. H. Cho, J. H. Park, K. B. Kwon, Y. R. Lee, H. S. So, K. K. Lee, S. Y. Lee, S. R. Moon and S. H. Yang, Autophagy induction by low-dose cisplatin: The role of p53 in autophagy, *Oncol Rep*, 2014, **31**, 248-254.

32 T. Wu, M. C. Wang, L. Jing, Z. Y. Liu, H. Guo, Y. Liu, Y. Y. Bai, Y. Z. Cheng, K. J. Nan and X. Liang, Autophagy facilitates lung adenocarcinoma resistance to cisplatin treatment by activation of AMPK/mTOR signaling pathway, *Drug Des Dev Ther*, 2015, **9**.

33 S. Chouaib, M. Z. Noman, K. Kosmatopoulos and M. A. Curran, Hypoxic stress: obstacles and opportunities for innovative immunotherapy of cancer, *Oncogene*, 2016.

34 J. P. Cosse and C. Michiels, Tumour hypoxia affects the responsiveness of cancer cells to chemotherapy and promotes

cancer progression, *Anticancer Agents Med Chem*, 2008, **8**, 790-797.

35 M. Hockel and P. Vaupel, Tumor hypoxia: definitions and current clinical, biologic, and molecular aspects, *J Natl Cancer Inst*, 2001, **93**, 266-276.

36 S. Strese, M. Fryknas, R. Larsson and J. Gullbo, Effects of hypoxia on human cancer cell line chemosensitivity, *Bmc Cancer*, 2013, **13**, 331.

37 J. Zhou, T. Schmid, S. Schnitzer and B. Brune, Tumor hypoxia and cancer progression, *Cancer Lett*, 2006, **237**, 10-21.

38 H. M. Wu, Z. F. Jiang, P. S. Ding, L. J. Shao and R. Y. Liu, Hypoxia-induced autophagy mediates cisplatin resistance in lung cancer cells, *Sci Rep*, 2015, **5**, 12291.

39 N. M. Mazure and J. Pouyssegur, Hypoxia-induced autophagy: cell death or cell survival?, *Curr Opin Cell Biol*, 2010, **22**, 177-180.

40 M. Tafani, L. Sansone, F. Limana, T. Arcangeli, E. De Santis, M. Polese, M. Fini and M. A. Russo, The Interplay of Reactive Oxygen Species, Hypoxia, Inflammation, and Sirtuins in Cancer Initiation and Progression, *Oxid Med Cell Longev*, 2016, **2016**, 3907147.

41 N.J. Blackburn, Nan Yan, and S. Lutsenko, *Binding, Transport and Storage of Metal Ions in Biological Cells*, ed. W. Maret and A. Wedd, Royal Society of Chemistry, Cambridge (UK), 2014,**18**, 524-555.